

# Journal of Materials Chemistry B

Accepted Manuscript



This is an *Accepted Manuscript*, which has been through the Royal Society of Chemistry peer review process and has been accepted for publication.

*Accepted Manuscripts* are published online shortly after acceptance, before technical editing, formatting and proof reading. Using this free service, authors can make their results available to the community, in citable form, before we publish the edited article. We will replace this *Accepted Manuscript* with the edited and formatted *Advance Article* as soon as it is available.

You can find more information about *Accepted Manuscripts* in the [Information for Authors](#).

Please note that technical editing may introduce minor changes to the text and/or graphics, which may alter content. The journal's standard [Terms & Conditions](#) and the [Ethical guidelines](#) still apply. In no event shall the Royal Society of Chemistry be held responsible for any errors or omissions in this *Accepted Manuscript* or any consequences arising from the use of any information it contains.

## Mimicking biological phenomena in hydrogel-based biomaterials to promote dynamic cellular responses

Nicholas P. Murphy and Kyle J. Lampe

### Introduction

The extracellular matrix (ECM) was long thought of as simply an inert structural support inside of which cells self-regulate their activity. Prior to 1980, the field of cell biology had accepted that cells alone contain all of the inherent biological phenomena sufficient to create mature tissues<sup>1</sup>. The recognition of integrins in 1987 as prominent cell adhesion molecules<sup>2</sup> sparked the study and discovery of many other cell adhesion molecules<sup>3-5</sup> forever altering the consensus view of the ECM. These linkages between cells and their ECM promote adhesion, transduce mechanical force, and initiate signals both from the cell to the ECM, such as secreted proteases and mechanical stretching of ECM proteins, and from the ECM to the cell, such as released growth factors and countering forces via cytoskeletal reorganization. The importance of ECM on cell viability and activity is evident in a recent review that summarized ECM reorganization and loss of function<sup>1</sup>. As one example, the loss of fibronectin is lethal to the developing embryo, partially due to insufficient morphogenesis during defects in neural tube formation. We now know that the ECM is not present to simply hold cells in place, an unchanging background in which cells simply exist. It is an active, temporally and spatially organized, environmental template that continuously influences and responds to the embedded cells. Furthermore, the ECM's bioactivity does not just come from the sequestered signaling molecules such as soluble growth factors. It is in and of itself a potent signaling molecule.

A classic example of ECM bioactivity is seen in the provisional wound matrix of the wound healing response. The provisional wound matrix acts to trap growth factors that guide regenerative cells to the site of injury and to stimulate the cells to transition into regenerative phenotypes undergoing proliferation, differentiation, and/or synthesis and deposition of new matrix. The provisional matrix is an insoluble fibrin clot initiated by thrombin cleaving fibrinogen. Growth factors secreted by platelets including platelet-derived growth factor (PDGF), transforming growth factor beta (TGF- $\beta$ ), and fibroblast growth factor (FGF) are sequestered in the matrix, and act as chemotactic cues to promote fibroblast infiltration<sup>6</sup>. Fibroblasts then modify their integrin receptors, generating a phenotypic change from migrating fibroblasts to proliferating, regenerative fibroblasts. The change in fibroblast integrin receptor profile as well as the ability for fibroblasts to migrate through the matrix is dependent on the presence of fibrin<sup>7</sup>. Aside from depositing new ECM molecules, the cells secrete matrix metalloproteinases (MMPs) to specifically remove injury-degraded ECM molecules, while MMP-inhibitory tissue inhibitors of metalloproteinases (TIMPs) are simultaneously secreted to ensure that functional ECM molecules are not degraded. This elegant cell-ECM control loop serves to clearly show the importance of the ECM in its stimulation of cell activity.

Mechanical and biochemical facets from the native ECM can be incorporated into user-defined hydrogel materials to stimulate cells with an environment conducive to a given regenerative application. Some of the earliest examples of this biological incorporation are grafting full enzymes onto a polymer membrane<sup>8</sup> and crosslinking a synthetic polymeric material with protease-cleavable polypeptides such as poly(2-hydroxyethyl-L-glutamine)<sup>9</sup>. As discussed later, hydrogels can be made completely from native ECM molecules to impart bioactivity through already present adhesion domains and protease cleavable sites. To promote a desired cellular response, researchers often pursue more controllable materials where they can independently tune variables such as material stiffness and biochemical ligand presentation. The seminal work of Discher and coworkers suggested that stem cell fate is a direct result of the substrate stiffness. Differences in polyacrylamide (PA) substrate stiffness led to completely altered gene expression profiles in mesenchymal stem cells (MSCs), with neurogenic differentiation selected at low stiffness, myogenic differentiation selected at medium stiffness, and osteogenic differentiation selected at high stiffness<sup>10</sup>. This result may in part be due to the manner in which ECM proteins were tethered to the substrate surface, as stiffness-dependent cell fate was later shown to be at least partly a result of lower density of ECM docking sites as substrate stiffness decreases (and porosity increases)<sup>11</sup>. More recent work found that MSC fate is a product of substrate stiffness alone and not ECM protein tethering<sup>12</sup>.

In addition to human MSCs (hMSCs) which can differentiate into many tissue types, the fates of hematopoietic stem cells (HSCs)<sup>13</sup> and neural stem cells (NSCs)<sup>14, 15</sup> are confined to blood cell types and neural cell types, respectively. These “tissue-specific” stem cells maintain activity when surrounded by matrices having mechanical properties similar to their native tissue. The viability and neuronal differentiation of NSCs encapsulated within 3D hydrogels has been shown to be maximized at moduli mimicking native brain tissue<sup>16-18</sup>. Matrix dimensionality is also a critical variable for cell survival and activity, as sensory neurons display native morphological phenotypes on 3D matrices, but not on 2D matrices<sup>19</sup>. 3D environments are also sufficient for matrix deposition<sup>20</sup> while 2D environments are not<sup>21</sup>. Similarly, Lampe and coworkers found that the neurite outgrowth of dorsal root ganglion neurons (DRGs) in 3D is maximized at moduli similar to their native environment (~0.5 kPa) while higher moduli are increasingly inhibitory to neurite outgrowth and viability (Figure 1A). Incorporation of the arginine-glycine-aspartate (RGD) adhesion motif from fibronectin into the scaffold similarly stimulated enhanced neurite outgrowth (Figure 1B). RGD incorporation provided encapsulated cells with a direct way to sense and respond to the mechanical properties of their surrounding matrix designed for the application of regenerating neural tissue<sup>22</sup>.

Acting as a set of tissue-specific dynamic microenvironments, the native ECM is invariably undergoing cell-mediated reconstruction through matrix deposition and degradation. As cells develop, bioactive ECM domains are temporally presented to cells both statically or dynamically. Mechanical properties of the ECM, such as stiffness and porosity, also change over time as cells develop. Biological factors such as growth factors or signaling molecules are released by cellular demand from the ECM. Soluble biomolecules are also secreted and degraded by cells, and can in some

cases bind to the ECM itself via fibronectin, as one example<sup>23</sup>. The inherent complexity of the native ECM provides a challenge in fabricating an ideal, completely bio-mimetic hydrogel material for cell culture and tissue regeneration. However, synthetic materials have been used to provide a template to introduce specific ECM moieties in order to determine individual or combinatory contributions. Partially synthetic materials are ideal for fabricating cell-responsive materials because *all* of the bioactivity can be user-defined and tuned as needed. We describe here efforts in which hydrogel materials were imparted with discrete bio-mimetic functionalities such as dynamic stiffening, growth factor presentation, and cell-mediated degradation to stimulate encapsulated cells to differentiate, proliferate, or stretch. Before hydrogel materials are introduced, we provide a perspective on the native biological phenomena that lays the groundwork for tissue-mimetic materials design.

## Biological framework for materials design

### *ECM composition and regulation*

The ECM is a highly dynamic environment whose set of molecules act as a code interpreted and edited by local cells. The ECM is a tapestry of different molecules including fibrous proteins like fibronectin, collagens, laminins, vitronectin and elastin; specialized proteins like growth factors, heparin, and integrin-binding glycoproteins; polysaccharides like glycosaminoglycans (GAGs) and HA; and proteoglycans like chondroitin sulfate proteoglycans (CSPGs)<sup>24</sup>. Different ECM molecules can have varying effects on cellular processes such as adhesion. For example, laminin and CSPGs play an important role in axon guidance as the former is stimulatory to neurite migration<sup>25</sup> and the latter is inhibitory to neurite migration<sup>26</sup>. CSPGs can be targeted by GAG-degrading chondroitinases to allow neurite sprouting and growth in spinal cord injury<sup>27</sup>; this phenomenon could potentially be modeled in an engineered hydrogel system (Figure 2A). Besides regulating cells, the ECM can also regulate itself. The production of one ECM molecule can be up- or down-regulated in response to the presence of another ECM molecule<sup>28</sup>. This mesh of molecules creates a matrix with a bulk stiffness sensed by cells through mechanotransduction followed by matrix tension signaling to cells via integrin linkages mediated by the Rho/Rho-associated protein kinase (ROCK) signaling cascade, which can regulate cell fate decisions important in wound repair. For instance, as the matrix contracts protein kinase B (Akt) is dephosphorylated, converting a survival signal into an apoptotic signal<sup>29, 30</sup>. As another example, matrix-mediated changes in cell shape can activate Ras homolog gene family, member A (RhoA) signaling, and can regulate osteogenic differentiation<sup>31</sup>.

The ECM can sequester and release many stimulatory factors: signaling molecules like amphiregulin and Wnts, growth factors such as TGF- $\beta$  and FGF, and also cell-mediated ECM cleavage fragments. The NC1 domain from collagen, a degradation fragment, stimulates neuronal axon growth<sup>32</sup> (Figure 2B). Cell-secreted TGF- $\beta$  interacts with latent TGF- $\beta$  binding protein (LTBP) to form large latent complexes (LLCs). TGF- $\beta$  is released from the ECM upon cell contacts applying force to the ECM, uncoupling the LLCs<sup>33</sup>. In this way, TGF- $\beta$  signaling can be tuned by the

rigidity and composition of the ECM. Normal and disease-state remodeling of the ECM by cellular degradation can also affect cell morphology and movement. This often takes place through MMPs that can cleave ECM proteins, thereby reducing the crosslinking density of the matrix (and therefore changing the stiffness which has impact previously discussed) and potentially opening “highways” for cell migration. For example, osteoblast-secreted MMP-9 releases Kit Ligand from the matrix, which interacts with the Kit tyrosine kinase receptor on hematopoietic stem cells (HSCs), creating a signal triggering HSC locomotion<sup>34</sup>.

### *Cellular adhesion and migration*

The ECM can act as a docking site for cell adherence and migration via adhesion receptor binding and unbinding, providing an additional means to signal to encapsulated cells. All cellular adhesions involve cell surface receptors like integrins, selectins and cadherins, and interactions with the actin cytoskeleton. Integrins are transmembrane receptors for ECM molecules and are critical for cell-matrix adhesion. There are three main classes of adhesions: (1) focal adhesions<sup>35</sup>, (2) focal complexes<sup>36</sup>, and (3) fibrillar adhesions<sup>37</sup>. Focal adhesions, flat structures that are regulated by RhoA and actomyosin contractility, involve anchoring of actin microfilaments that mediates strong adhesion to the matrix. Focal complexes, dot-like precursors to focal adhesions, are induced by the Rho-family GTPase Rac. Fibrillar adhesions can be long or dot-like structures, and involve adhesion via ECM fibrils. Many types of molecules are involved in cellular adhesion, including integrins, adhesive non-integrin molecules such as syndecan-4 and urokinase receptor (uPAR), and integrin-actin linkers such as focal adhesion kinase (FAK), down-regulated in rhabdomyosarcoma LIM protein (DRAL), and integrin-linked kinase (ILK). Cell adhesion is a product of probing for mechanical forces. Once attached, focal adhesions provide a means to exert countering forces onto the matrix<sup>38</sup>. There are many biochemical ways for cells to respond to mechanical stimuli including cell adhesion receptors, stretch-activated ion channels<sup>39</sup> and mechanically gated ion channels<sup>40</sup>.

The ECM is not just a structural scaffold but also a bioactive director. As already discussed, the fibronectin-derived RGD sequence promotes cell adhesion and is responsible for mediating fibronectin fibrillogenesis. In the context of native ECM, this can lead to fibroblast stimulation and myofibroblast and macrophage migration into a wound site covered topically with adhesion-site-rich fibronectin. On the opposite end of the spectrum when fibronectin is knocked-down, myocardial precursor migration is completely eliminated leading to cardia bifida<sup>41</sup>. In another example of ECM activity fibrillar collagen can ligate and phosphorylate mammary gland receptor tyrosine kinases<sup>42</sup>. Covalent modifications can be made to the ECM by cell-secreted molecules such as growth factors that bind to heparin<sup>43</sup> and through biological crosslinking via the transglutaminase factor XIIIa<sup>44</sup>. When ECM makeup is heterogeneous, gradients in ECM composition can lead to gradients in cell locomotion velocity. For example, neural crest cells will migrate significantly faster on versican-containing matrix than aggrecan-containing matrix<sup>45</sup>. In some cases, as in epiblastic cell movement during primitive streak formation, cells can ‘carry’ their



ECM along their migration<sup>46</sup>. Thus, the ECM is not set in its location as it is also not set in its composition and mechanical properties.

### *Cryptic domains and ECM remodeling*

One way for cells to remodel their environment is to mechanically alter their local matrix. Fibronectin fibrillogenesis is an important integrin-mediated phenomenon that involves soluble fibronectin components transitioning to insoluble fibrillar fibronectin (Figure 2C). Fibronectin can initiate its own multimerization, but the respective domains are “cryptic” such that they are hidden in fibronectin’s stable, globular state mostly within its FNIII domains<sup>38</sup>. Cryptic sites can be unearthed by either mechanical stretching<sup>47</sup> or proteolytic cleavage<sup>48</sup>. Simulations have led to predictions of a ‘multimerization sequence’ and experimental work has distilled these predictions to a seven-amino-acid sequence sufficient to induce multimerization. The proposed multimerization sequence, termed ‘CPB’ and having the primary structure SLLISWD, was experimentally shown to be cryptic and to interact with fibronectin in a manner that exposes other cryptic hydrophobic domains<sup>49</sup>. As important domains involved in fibronectin fibrillogenesis are now known, it is possible for biomaterials engineers to begin thinking about how to controllably induce fibril formation of native or engineered ECM via cell stretching. Aside from associating with itself, fibronectin interacts with other ECM molecules including tenascin<sup>50</sup>, CSPGs<sup>51</sup>, heparin<sup>52</sup> and hyaluronic acid<sup>52</sup>. Fibronectin-ECM interactions can be both inhibitory<sup>53</sup> and stimulatory<sup>54</sup> to cell-ECM adhesion.

Before fibrillogenesis, secreted fibronectin must be unfolded in order for it to polymerize. The actin cytoskeleton and signaling effectors are essential for this process<sup>24</sup>. Fibronectin fibrillogenesis is tightly regulated in native environments; this regulation seems to be lost in diseased environments. Tumor cells give rise to extra-stiff ECM, and this is partly due to increased unfolding of fibronectin<sup>55</sup>. Fibronectin fibrillogenesis is not only a product of cellular forces, but can also result from cell-independent mechanical forces and thus from the surrounding matrix. Fibronectin can stretch and subsequently multimerize on different materials. Garcia and coworkers showed that soluble fibronectin can spontaneously form fibrils on a poly(ethyl acrylate) substrate but not on a poly(methyl acrylate) substrate, with myogenic differentiation of murine C2C12 myoblasts enhanced on the former material<sup>56</sup>. Biomaterials engineers may thus design matrices that utilize cell- or matrix-derived mechanical forces to control matrix fibril formation.

The length scales and heterogeneity of fibronectin remodeling limits the use of high-resolution fluorescent microscopy to 2D surfaces. To combat the length scale and time scale challenges of monitoring fibronectin remodeling, the Vogel group developed microfabricated tissue gauges ( $\mu$ TUGs) that can be combined with fluorescence resonance energy transfer (FRET) to observe high resolution 3D remodeling of user-supplied, cell-assembled fibronectin onto a polymerized collagen scaffold. Collagen-colocalized multimerized fibronectin was observed to be compact and progressively unfolded, with bidirectional strain gradients appearing. The role of fibronectin seems to change with time of incorporation into the scaffold.

Fibronectin that is incorporated early into the matrix is mostly compact and acts to stabilize the initial structure, while fibronectin assembled later are stretched by cells and multimerized (Figure 3A) corresponding to increased matrix tension (Figure 3B)<sup>57</sup>. Information about the spatio-temporal remodeling of ECM proteins can help with design of *in vivo* injury interventions or biomaterial implantations where force-mediated remodeling is a critical design feature.

## Hydrogels as tissue-like biomaterials

Native tissue is characterized by high water content, and therefore hydrogels composed of hydrophilic polymers, synthetic or natural, present good models conducive to transport of exogenous or cell-derived bio-factors. Purely synthetic hydrogels can promote healing phenotypes such as tunable differentiation, proliferation and migration, based off of mechanical properties alone, but it is the dynamic marriage of mechanical and biochemical properties that is a hallmark of native tissue, behavior now pursued in tissue engineering strategies. Biochemical motifs such as growth factors, cytokines, and chemotactic gradients can be incorporated and tightly tuned within a hydrogel<sup>58</sup>.

Here we describe two classes of therapeutic hydrogels: (1) purely natural and (2) partially-synthetic materials. While synthetic materials are frequently referred to as “inert” they often have specific bioactivity that can be beneficial<sup>59</sup> or inhibitory<sup>60</sup>. Purely synthetic materials can give insight into natural phenomena such as ECM-composition-dependent cell maturation. For example, cardiomyocytes derived from human induced pluripotent stem cells (iPSC-CMs) exhibited the largest mitochondrial function and intermediate filament gene expression on a 4% PEG-96% PCL material relative to other compositions<sup>61</sup>. Synthetic materials need not incorporate cell-interactive elements to abate scarring and an engulfing phagocytic response<sup>62, 63</sup>, but these cell-interactive elements are desirable to promote tissue regeneration within a hydrogel environment.

### *Purely natural hydrogelling materials*

Materials derived from natural sources serve as a model that can inherently mimic the native extracellular milieu. Cell culture studies incorporating natural scaffolds have allowed researchers to gain an understanding of the complex action of the native ECM. Purely natural materials have been used to deliver cells and as a means for cell infiltration to promote *in vivo* matrix remodeling<sup>64</sup>. We will discuss here ECM-derived materials that have been successfully used in a modified format (i.e., attachment of biomolecules).

Collagen type I is the most abundant protein in the majority of tissue matrices and is widely used for regenerative purposes because it contains numerous domains for adhesion of cells as well as to other ECM molecules like fibronectin. The triple-helical structure of gelled collagen type I proceeds via pH- and temperature-induced multimerization of a monomer solution. Collagen is a physical hydrogel and mechanically weak material, but can be strengthened by chemical glycation<sup>65</sup> or a secondary crosslinking mechanism<sup>66</sup>. Biomolecules can be

covalently or non-covalently introduced into a collagen scaffold via natural interactions<sup>43</sup>, collagen-binding sequences recombinantly engineered into a protein<sup>67</sup> or by chemical coupling<sup>68</sup>. Collagen from animal sources has led to adverse immunogenic reactions *in vivo*<sup>69</sup>, prompting the use of recombinantly-derived collagen<sup>70</sup>. Gelatin is a denatured form of collagen and gels similarly in tissue culture<sup>71</sup> or protein delivery<sup>72</sup> applications. Another widely used material for its role in clotting and tissue regeneration, fibrin, is derived from the polymerization of fibrinogen with thrombin and is recognized by many cell-adhesion receptors<sup>73</sup> and contains many covalent crosslinks susceptible to proteases<sup>74</sup>. Thus, cell migration through fibrin occurs almost exclusively via proteolytic degradation. Fibrin can be covalently functionalized by crosslinking with a protein incorporating a transglutaminase domain via its natural polymerizer, the transglutaminase factor XIIIa<sup>75</sup>. Un-modified fibrin has been used in a rat model of spinal cord injury to promote neural fiber and astrocyte infiltration into the lesion site<sup>76</sup> (Figure 4).

A non-protein material, HA is an anionic linear glycosaminoglycan composed of D-glucuronic acid and N-acetyl-D-glucosamine that can be produced by bacterial fermentation. HA has been used for the repair of cartilage<sup>77</sup>, bone<sup>77</sup>, and vocal cord<sup>78</sup>, as well as for angiogenesis<sup>79</sup>. HA hydrogels take in much water due to their anionic character and thus have weak mechanical properties. However, direct modifications of its functional groups with more hydrophobic moieties have resulted in HA hydrogels with diverse mechanical properties<sup>80,81</sup>. HA is unable to bind to integrins and is slowly degraded by the protease hyaluronidase, thus HA materials have been modified with cell-adhesion ligands<sup>82</sup> and protease-cleavable sequences<sup>83</sup>. Hydrogels based off of a blend of HA with methylcellulose termed HAMC have become a novel means to transport regenerative retinal stem-progenitor cells into the degenerating retina<sup>84</sup>.

Alginate, while grouped here as a natural material since it is extracted from seaweed, is the only natural material in this section not natively present within the human body. Despite that, alginate has been used in numerous clinical applications including as a wound healing dressing<sup>85</sup> and as a drug<sup>86</sup> and cell<sup>87</sup> carrier. Alginate is an anionic polysaccharide composed of  $\beta$ -D-mannuronic acid and  $\alpha$ -L-gluronic acid that can be crosslinked via divalent cations, typically  $\text{Ca}^{2+}$ ,  $\text{Mg}^{2+}$ , or that create inter-macromer bridges between the gluronic acid groups<sup>88</sup>. Alginate is regularly used to create tunable viscoelastic hydrogels but perhaps due to its source, does not have inherent biological activity. Alginate has been modified in a number of ways discussed further below, to endow it with enhanced crosslinking and cell-interactive functionality. Covalent crosslinking can also be performed with multi-functional molecules such as poly(ethylene glycol) (PEG)-diamines to improve durability and increase stiffness<sup>89</sup>. To incorporate biomolecules, the carboxylic groups of alginate sugar residues can be crosslinked to peptides via amide linkages<sup>90</sup>.

### *Partially Synthetic Materials*

Purely synthetic materials inherently do not have any specific bioactive domains, but their mechanical properties are sufficient to promote biological responses such as stiffness-dependent differentiation or as a surface for cells to



attach, as is the case with polyornithine. Engineering single or multiple biological components into a synthetic material can be useful to obtain a desired cellular response or to understand the contributions of a particular biomolecule. The RGD adhesion site from fibronectin has been widely used in partially synthetic materials to allow cells to dock with the scaffold and establish forces necessary for spreading and differentiation. RGD incorporation into an elastin-like polypeptide (ELP) scaffold enhanced neurite outgrowth of encapsulated DRGs<sup>22, 91, 92</sup>.

The classic RGD sequence from fibronectin is the most frequently used, but other adhesion sites from other ECM molecules have been identified including IKLLI, IKVAV, LRE, PDSGR, and YIGSR<sup>93, 94</sup> from laminin as well as DGEA from collagen. IKVAV and IKLLI had the greatest effect on PEG-encapsulated  $\beta$ -cells, resulting in significantly increased survival and higher insulin production relative to other peptides<sup>95</sup>. There is also evidence of synergistic effects of multiple adhesive peptides, such as PDGSR and YIGSR on glucose-stimulated insulin release<sup>95</sup>, RGD and IKVAV on human umbilical vein endothelial cell (HUVEC) growth<sup>96</sup>, as well as antagonistic effects such as RGD and YIGSR on HUVEC cell growth<sup>96</sup> and PC12 cell neurite extension<sup>97</sup>. Full-length proteins can be covalently conjugated into synthetic gels that display appropriate end groups. Conjugation of laminin into a PEG-N-hydroxysuccinimide (NHS) hydrogel resulted in increased neurite extension of encapsulated DRGs<sup>98</sup>. For delivery applications, oxidized antibodies can be covalently attached to a hydrogel consisting of HA with adipic dihydrazide end groups<sup>99</sup>.

### *Dynamic Materials*

While synthetic hydrogels provide a system in which static mechanical properties are easily tuned and user-defined, mechanically static materials are likely not the end-all solution regardless of enhancements by pendant biochemical moieties. The heterogeneity within a given tissue is increasingly recognized in current research with positional tissue stiffness gradients existing in mature eukaryotes<sup>100</sup>. Analogously, there also exist gradients with respect to both space and time in eukaryotic tissue. For instance, a stiffness gradient in time and space is explicitly understood during development, wound healing and disease. As a classic example, the mature chicken heart has a stiffness of roughly 10 kPa; however, the originating mesoderm is a much softer  $\sim 0.5$  kPa material. Complete stiffening of the chicken heart takes approximately two weeks<sup>101</sup>. Fibrosis, a response in wound healing as well as after heart attack, is another example of natural tissue stiffening, but in this case to an unnatural, scar-like state<sup>102</sup>. Matrix stiffening is apparent in diseased states as well as aging and can contribute to corresponding adverse phenotypes. Amidst aging and progression of atherosclerosis, the blood vessel wall stiffens leading to increased endothelial cell permeability due to elevated cell contractility, thus widening cell-cell junctions<sup>100</sup>.

There have been recent developments in mimicking this dynamic stiffening of native ECM. Young and Engler have developed a stiffening material from thiolated hyaluronic acid (HA-SH)<sup>103</sup>. For these HA-SH materials, initial gelation is achieved by crosslinking with PEG-diacrylate (PEGDA). Further time-dependent stiffening is

then allowed to occur by free acrylate groups on the HA backbone polymerizing with leftover HA-SH groups from the initial crosslink reaction. They were able to create a material that stiffened from 1.9kPa to 8.2kPa over 19 days post-polymerization, corresponding to development of the native chicken heart. It should be noted that this temporal stiffening was not linear, but rather followed a decaying exponential, such that the majority of stiffening occurred after three days. The stiffening HA-SH hydrogel allowed for significantly improved pre-cardiac cell maturation into myocytes, as seen by a 3-fold increase in expression of the mature marker Troponin T as well as a significant increase in mature myofibrils, relative to cells cultured on a static PA material. However, the HA-SH materials are a liability *in vivo* as they caused a significant increase in macrophage and lymphocyte infiltration at the site of an intramyocardial injection. Follow up work attributes this immune response to the free thiol groups, since a non-thiolated HA did not cause an immune response<sup>104</sup>; however, the process of stiffening may also contribute.

Guvendiren and Burdick have more recently developed methacrylated HA (Me-HA) based hydrogels that are capable of stiffening in a stepwise manner<sup>105</sup>. For initial gelation, methacrylate groups were crosslinked with dithiothreitol (DDT). At a user-defined time point later, further crosslinking of unreacted methacrylates can be induced by addition of UV light with a photoinitiator (Figure 5A,B). Switch-like stiffening can alter the fate of uncommitted precursors (Figure 5C), and the composition of cell types in a bi-potential media can be tuned by varying the time of further stiffening. For hMSCs cultured on Me-HA hydrogels in a bipotential media promoting osteogenesis and adipogenesis, osteogenic markers were more apparent for materials stiffened at earlier time points, and adipogenic markers were more apparent for materials stiffened at later time points. This fate-tuning is realized because differentiating cells do not respond to mechanical stimuli, as do uncommitted cells. By using hydrogels that incorporate switch-induced stiffening like the Me-HA based materials, it is possible that the exact fate and composition of uncommitted progenitors or stem cells could be tuned and induced at a user-defined time point<sup>105, 106</sup>.

Bioactive peptide domains can be introduced into the scaffold to mimic native dynamic presentation. For instance, hMSCs early during their differentiation into chondrocytes upregulate fibronectin production thus providing increasing RGD domain concentration. One week after differentiation, fibronectin is downregulated, freeing the cells to a more spherical morphology necessary for chondrogenic differentiation. To recapitulate this dynamic native RGD presentation, the Anseth group designed a peptide sequence incorporating RGD as well as a MMP-13-cleavable sequence (PENFF)<sup>107</sup>. This peptide design was realized because MMP-13 is upregulated in chondrocytes as fibronectin is downregulated. Upon incorporating this peptide into a PEGDA hydrogel, RGD could be cleaved on a physiological time scale specifically by cell-secreted MMP-13, and the appropriate hMSC response was observed – initial adhesion followed by detachment.

Researchers are now utilizing light irradiation to induce user-defined temporal and spatial degradation gradients in synthetic materials crosslinked with photo-labile bonds. Near-infrared-light irradiation was used to trigger release of various neurotransmitters such as dopamine from polypyrrole nanoparticles in

order to remote-control brain activity<sup>108</sup>. In a further iteration of the temporal RGD presentation design, RGD was attached to the backbone of a PEGDA scaffold via a photo-cleavable bond, resulting in a hydrogel in which RGD could be released at user-defined times to enhance chondrogenic differentiation<sup>109</sup>. Unlike with cell-demanded matrix degradation, the researcher can tune the cellular microenvironment with micron-scale resolution to understand how cells respond to such changes. The decrease in crosslink density that arises from photodegradation results in an increased porosity of the material advantageous for cell spreading and diffusion of secreted molecules. In photo-labile hydrogels encapsulating hMSCs, a light-induced polymer density gradient supported a corresponding gradient in hMSC spreading and area<sup>110</sup>.

Porosity may also be a desirable variable to temporally tune in a hydrogel system. A low-porosity material may provide an initial barrier to protect fragile precursor cells from the outside environment; however, a more porous material is required for the diffusion of growth factors, cell spreading and migration, matrix deposition, and angiogenesis. Thus, the design of a time-dependent increase in hydrogel porosity is attractive. A scaffold composed entirely of MMP-degradable, RGD-presenting spherical microgels that anneal via factor XIIIa, termed microporous annealed particle (MAP) gels, was designed to attain microporosity upon cellular degradation of the microgels<sup>111</sup>. Compared to non-porous PEG-VS scaffolds, the MAP gels showed increased cellular network formation, proliferation, wound closure, and a decreased immune response. Advancing on this work is a methacrylated-gelatin-based material implementing three porogens that degrade in response to different stimuli<sup>112</sup>. Compared to one and two sequential treatments, collagen II and X deposition was markedly increased in the thrice-treated hydrogel and cell density was increased in the twice-and thrice-treated hydrogel.

These control features of step-changes in either stiffness or porosity are useful new tools that allow researchers to understand and direct cell fate *in vitro*. However, they lack broad clinical applicability due to the added challenge of accessing the implantation site to provide the stimulus/trigger to cause the desired change. These designs are sufficient for proof-of-concept applications, but materials are ultimately needed to provide all necessary bioactivity without necessitating user input, and surgical access, after implantation. Materials that are inherently bioactive, designed to respond to cellular inputs like protease secretion or cell stretching, are ultimately what are needed.

### **Bio-responsive release and degradation**

Biomaterials engineers hope to take advantage of cell-mediated matrix degradation as a design strategy that builds into the system an ability for encapsulated cells to “talk” to their surrounding matrix. This communication can include matrix degradation via cell-secreted proteases coupled with other cell-matrix interactions that dictate fate decisions. Materials that cell-responsively degrade are important to the regenerative capacity of encapsulated cells: presentation of non-degradable crosslinks negatively directs cell fate and blocks traction force generation in a manner analogous to myosin inhibition<sup>106</sup>. In

applications where protease activity is detrimentally upregulated such as after a myocardial infarction, materials can be designed to provide feedback on cell-mediated degradation<sup>113</sup>.

### *Growth Factor Delivery*

Designing a material to release stimulatory factors in response to cell inputs “on demand” will be more useful than in response to user-dictated, extrinsic inputs. This allows cells to customize their environment with factors available as needed during development rather than at step-change intervals convenient to researchers. One natural cell input that could induce growth factor release is degradation, realized with bulk material-sequestered factors (bulk degradation) or factors covalently attached to the scaffold via a tether (tether degradation). Freedom of design is available in either method – protease-sensitive sites in the bulk material backbone can be cleaved to release sequestered growth factors, or growth factors can be tethered to the scaffold by Michael-type addition with free acrylate groups. When using synthetic macromers for hydrogel formation, the choice of crosslinking-active end groups is important for the degradation application. For example, crosslinking PEG acrylates will form ester bonds cleaved over time by hydrolysis, while crosslinked PEG vinyl sulfones (PEG-VS) will not degrade in response to water<sup>114</sup>. Incorporation of protease-cleavable substrates into the latter hydrogel will result in cell-mediated degradation as the sole mechanism of remodeling<sup>115</sup>. This situation is ideal for immobilizing growth factors, as their degradation-mediated release can be cell-responsive in both time and space (Figure 2D).

Multiple growth factors may need to be delivered in some clinical applications where matrix degradation and remodeling are important to healing, and in some cases, proteases can have multiple regulating growth factors. Exogenously added growth factors can work in concert with natural ECM- and cell-derived cues. A PEG-VS hydrogel crosslinked with a bifunctional vascular endothelial growth factor (VEGF) protein and pendant, engineered RGD peptide significantly increased cell migration relative to the control without the adhesion peptide<sup>116</sup>. The presence of VEGF stimulated HUVEC production of latent MMP-2, subsequently activated by sequestered TGF- $\beta$ 1. Thus, VEGF and TGF- $\beta$ 1 can work together in an engineered hydrogel system to mediate HUVEC synthesis *and* activation of MMP-2.

Zisch and coworkers used a 4-arm PEG-VS hydrogel crosslinked with free thiol-bearing MMP-sensitive peptides, and plasmin-sensitive VEGF variants including VEGF<sub>121-Cys</sub> (Figure 6A) were attached as pendant molecules via Michael-type addition<sup>117</sup>. Encapsulated HUVECs showed similar radial outgrowth with the bound growth factor and with the soluble form. When these hydrogels were grafted onto a chicken chorioallantoic membrane, a highly localized blood vessel growth response was seen at the graft site, a result not seen in hydrogels with soluble or no VEGF (Figure 6B). Delivering growth factors in the form of molecules bound by a protease-cleavable tether can result in a highly localized source, critical for angiogenesis<sup>117</sup>.

Cell-mediated ECM degradation can also facilitate the delivery of drug-delivering nanoparticles that can cross the cell membrane. Nanoparticles can be conjugated to a PEG scaffold through the biotin/streptavidin complex<sup>118</sup>. To facilitate released based on cellular inputs, end-thiolated protease-cleavable peptides were attached to nanoparticles via maleimide chemistry. Release rates were tuned not only by peptide sequence but also by degree of peptide modification, with fewer tethers per nanoparticle resulting in a faster release. Aside from the coupled growth factor delivery with matrix degradation, nanoparticles permanently tethered to the scaffold could provide a sustained release of encapsulated growth factors.

Many protein growth factors bind to heparin with high affinity, providing another means to sequester growth factors to the scaffold. This phenomenon has prompted the use of bound heparin as a means to sequester exogenously supplied growth factors for either passive or cell-demanded release realized by heparinase. Mathematical modeling incorporating material balances utilizing association/dissociation rate constants for basic fibroblast growth factor (bFGF) binding to heparin yielded optimal conditions such that passive release is much slower than cell-demanded release. A 500-fold molar excess of heparin to bFGF was the optimal condition, leading to a 2-fold increase in neurite extension of DRGs<sup>119</sup>.

### *Peptide Design*

Peptides linked into a hydrogel system allow a broad design space to control many variables that are part of the bulk material properties or cell response. Foremost, a peptide can be designed to crosslink with the polymer. To allow crosslinking and subsequent gelation with acrylate or vinyl sulfone groups, peptides can be designed with cysteines or lysines on each end. Thiols are present in proteins naturally but are usually in the form of disulfide bridges; crosslinking with these thiols could denature the protein. Designing recombinant proteins is a useful tool for engineering crosslinkable peptides into the scaffold. Proteolytic degradation depends on protease activity, adhesion ligand concentration, and matrix crosslink density<sup>115</sup>. Depending on the peptide used, sensitivity to a particular protease or multiple proteases can be designed into the material, which could be useful for specific applications. For example, urokinase-type plasminogen activator (uPA) is a protease secreted from the tips of growing neurites. A hydrogel made from ELPs composed of uPA-sensitive sites and adhesion sequences aided neuronal differentiation<sup>120, 121</sup>.

Enzymatic crosslinking is an option that can provide non-cytotoxic crosslinking as well as site-specificity. For example, the coagulation factor XIIIa catalyzes the acyl-transfer between the  $\alpha$ -carboxamide group of glutamines and the  $\epsilon$ -amino group of lysines. To facilitate factor XIIIa-induced crosslinking, peptides can be designed with the glutamine acceptor NQEQVSPL<sup>122</sup> (Figure 6 C,D). It may be desirable to control the susceptibility to a particular enzyme since particular proteases are upregulated during the wound healing response. The amino acid sequence of peptides can be tuned to control Michaelis-Menten kinetics. By changing the alanine in a natural collagen I-derived sequence to a tryptophan, the  $K_m$



decreased 1.5-fold and the  $k_{\text{cat}}$  increased 3-fold to MMP-1<sup>115</sup>. The kinetics are also a function of polymer molecular weight. Thus, a number of user-defined variables regarding protease-sensitive peptides can be tuned to control the rate of hydrogel degradation including amino acid sequence and bulk polymer molecular weight.

The rate of degradation and protease-sensitivity of materials presenting protease-cleavable substrates is very sensitive to the amino acid sequence of the peptide substrate. The collagen-derived substrates GPQG↓IAGQ or GPQG↓IWGQ are the most readily used to induce cell-mediated degradation, though these are relatively slow degrading and non-specific. Combinatorial methods using oriented peptide libraries as well as phage-display libraries have produced peptides with up to 600-fold increases in  $k_{\text{cat}}/K_{\text{M}}$  relative to GPQG↓IAGQ<sup>123</sup>. Secreted-protein-acidic-and-rich-in-cysteine (SPARC)-derived peptides have been identified to be cleaved mainly by plasmin, and show a broad range of kinetic parameters. When crosslinking a protease substrate into a hydrogel, the  $k_{\text{cat}}$  scales directly with hydrogel degradation rate. Since the  $k_{\text{cat}}$  values of many protease-sensitive peptide substrates have been studied and tabulated, it is now fairly simple to tune the cell-mediated degradation rate upon knowing the protease profile of the particular cell type in use<sup>124</sup>.

The ability of cells to locally degrade their surrounding matrix directly affects their locomotive capacity. Proteolysis is the usual primary mechanism to allow cell migration; however, if proteolysis is not an option, cells can adopt an amoeboid migration strategy. This mesenchymal-to-amoeboid transition has been shown to occur upon MMP activity inhibition, but only when the matrix porosity is large enough to sustain amoeboid migration. Cell migration through nanoporous fibrin is highly dependent on MMP modulation, while migration through porous collagen is independent of MMP activity modulation<sup>125</sup>. For all migrating cells, the cell speed is a result of a balance between the forces of adhesion and contraction. Inside of a given matrix system, the optimum speed of a given cell will stay constant upon reducing cell adhesivity (i.e. blocking integrin receptors) by increasing the matrix ligand density and decreasing the matrix stiffness<sup>126</sup>.

A new class of self-assembling peptides has been developed termed multidomain peptides (MDPs)<sup>127</sup>. These MDPs can form hydrogels at physiological pH and are designed to display user-defined length and functional domains. Charged residues can be carefully designed into the flanking regions to provide water solubility and oppose fiber assembly. Varying the number of flanking charged groups can control the stiffness. When an MMP-2 site was engineered into the core region of a MDP, the expected cleaved peptides were released as well as degradation products of released peptides. The combination of adhesion and degradation domains into the core region was shown to have a combinatory effect on cell spreading.

#### *Cell-triggered drug release from biomaterials*

The strategies discussed herein are not used exclusively to engineer new tissue. They are now frequently being adapted to create cell-responsive drug release

in native tissues. Biodegradable polymeric nanoparticles are broadly used in drug delivery because their release rate can be tuned and surface can be modified with protective groups or targeting ligands. For example, PEG can be attached to a particle surface to increase circulation time and diffusion through the brain parenchyma<sup>128</sup>. Drug release from polymeric nanoparticles and micelles remains a challenge as it is often too slow for clinical tumor therapy. Recent efforts have taken advantage of the intrinsic intracellular environment for faster drug release. Different chemistries have been deployed to prepare pH-sensitive nanoparticles based on acid-labile ortho ester<sup>129</sup>, hydrazone<sup>130</sup>, cis-aconityl<sup>131</sup>, and acetal<sup>132</sup> bonds. Bae and coworkers prepared micelles based off of an amphiphilic block copolymer containing a critical hydrazone-drug bond that would release the drug upon acidic, intracellular pH (Figure 7A,B)<sup>133</sup>. pH-sensitive drug delivery particles are design-limited because the pH difference between extracellular environment and the endosome is small. Incorporation of disulfide bond into the polymer chemistry will render degradation in the presence of high antioxidant content, such is the case in the cytosol where glutathione levels are approximately 2-10 mM. Chen and coworkers recently created a dual-responsive micelle, combining pH- and redox-sensitive motifs utilizing PEG-SS-poly(2,4,6-trimethoxybenzylidene-pentaerythritol carbonate)<sup>134</sup>. These two motifs – the acetal for pH sensitivity and the disulfide bond for redox sensitivity – resulted in a synergistic drug release effect. A diblock copolymer of PEG and polycaprolactone (PCL) linked by a disulfide bond capable of self-assembly showed markedly increased intracellular payload release relative to that without a disulfide bond<sup>135</sup> (Figure 7C,D).

Ligands with different functions can be attached to the surface of polymeric nanoparticles, or liposomes. Distinct ligands can be engineered to appear at varying, appropriate times during delivery. Longer PEG chains can shield other functionalities on a particle surface, like cell-penetrating peptides, until the cell-targeting antibody has helped the particle reach its target tissue<sup>136</sup>. The acid-labile hydrazine bonds used to attach the antibodies and long, shielding PEG chains cleave and release the functional particles into inflammatory regions with low pH. These “smart” drug delivery nanoparticles were shown to internalize into fibroblasts and astrocytoma cells, but only when the shielding PEG linkages were pH-cleavable. Gillies and coworkers developed also a “smart” shielding-mediated pH-responsive drug delivery system using a dendrimer as the vehicle<sup>137</sup>. This dendrimer was based on PEG with hydrophobic groups (2,4,6-trimethoxybenzaldehyde) attached to the periphery via acid-labile bonds (1,3-diol of serinol). This dendrimer was designed to shed its protective hydrophobic core upon acidic conditions, rendering the dendrimer surface hydrophilic, resulting in destabilization of the polymer and ultimately drug release.

Reactive oxygen species (ROS) are another key feature of inflamed environments. Newly designed poly(propylene sulfide) (PPS) increases in hydrophobicity when oxidized by converting to poly(propylene sulfoxide) and ultimately poly(propylene sulfone)<sup>138</sup>. PPS was used in combination with poly(N-isopropylacrylamide) (PNIPAAm) and poly(N,N-dimethylacrylamide) (PDMA) to synthesize an ABC tri-block polymer that was both thermo-responsive and bio-responsive, releasing drug in response to ROS<sup>139</sup>. Curcumin release from PPS

microparticles was shown to be dependent on ROS concentration, and both empty and loaded microparticles were cell-protective against ROS stress, indicating a free radical scavenging ability of PPS<sup>140</sup>.

“Charge-conversional polymers” can be used to create drug delivery carriers that switch from a negative to positive charge in the endosome. Cationic polyaspartamide derivatives were modified with cis-aconic anhydride to result in anionic groups linked via an acid-labile bond<sup>141</sup>. Upon endosomal uptake, the polyanions leave the complex, resulting in di-protonated modules capable of endosomal disruption. Later work incorporated disulfide moieties into the particle core to take advantage of the reductive cytosol<sup>142</sup>. In a growing theme, multiple tunable steps are attractive to both drug delivery and tissue engineering strategies, and recent technology developing a three-step sequential enzyme cascade created bioresponsive polymeric materials that change morphology<sup>143</sup>.

## Summary and Outlook

Native cells respond to many different mechanical and biochemical cues throughout their life cycle. It is our goal as biomaterials engineers to utilize complex, native biological phenomena to design predictable, repeatable, interactive hydrogel materials. We aim to have tunable design control of static and dynamic hydrogel materials. These should incorporate native biochemical and physical features in order to achieve a desired cellular response or set of responses over a specified regeneration time scale. Much success has come from work implementing biological factors such as recombinant, bound growth factors and protease-cleavable peptides into the scaffold backbone, and mechanical factors such as stiffening and dynamic porosity.

A future challenge in the field is to be able to tune what we call “indirect material responses.” For instance, as we have discussed, researchers commonly tune cell-mediated material degradation to control what fragments are to be cleaved and the time scale over which they are released. In native tissue, degradation fragments, such as the collagen degradation fragment NC1 domain, can play key roles in cellular development. How can we control the input to a cell from a pre-designed material? In some cases, cell-inputs from the material are only realized after cell stretching has revealed a cryptic domain. Can cryptic domains be engineered into partially synthetic materials to reproducibly examine the cellular response? Many cryptic domains have been identified such as the fibronectin multimerization sequences<sup>49</sup> and gelatin-binding site<sup>144</sup>. The cryptic fibronectin multimerization site is exposed upon mechanical stretching, and this has been applied in cell-free *in vitro* systems to fabricate assembled fibronectin matrices<sup>145</sup>. In native ECMs, there is a tight cell-mediated feedback mechanism in place to carefully control fibronectin multimerization<sup>55</sup>. Materials should be predictably remodeled by cells through a combination of different cell inputs including protease degradation and stretching to unveil a cryptic multimerization domain or channels/pores suitable for axon extension or cell migration. These remodeling events should then via a feed-forward input controllably induce a cascade of cellular responses.

Hydrogel materials in the future need not be designed to have a direct, one-step functionality, such as protease degradation leading to cellular migration. Rather, materials design incorporating multiple steps and multiple biochemical and mechanical phenomena will better mimic the complex native ECM<sup>146</sup>. A hypothetical situation could be: protease degradation leads to cellular migration to a new microenvironment via a chemotactic gradient where stimulatory factors are released conducive to proliferation. The cells begin to stretch the new matrix to reveal a cryptic domain that stimulates matrix-matrix bonding, increasing matrix stiffness, which then stimulates the cells to differentiate into mature, regenerative cell types. Finally, the material degrades to leave behind regenerative cells and their deposited matrix, thus closing the gap between proliferating precursors and tissue regeneration. The native ECM provides a “toolbox” of biological phenomena that can be engineered into biomaterials, some of which are highlighted in Figure 2. Materials that are designed beginning at the molecular level implementing carefully selected bioactive motifs that evolve and adapt in response to cell inputs will better mimic the native ECM and enable more regenerative clinical outcomes.

## References

1. T. Rozario and D. W. DeSimone, *Developmental Biology*, 2010, **341**, 126-140.
2. R. O. Hynes, *Cell*, 1987, **48**, 549-554.
3. S. D. Marlin and T. A. Springer, *Cell*, 1987, **51**, 813-819.
4. E. H. Fischer, H. Charbonneau and N. K. Tonks, *Science*, 1991, **253**, 401-406.
5. C. A. Buck and A. F. Horwitz, *Annual Review of Cell Biology*, 1987, **3**, 179-205.
6. D. Greiling and R. A. F. Clark, *J Cell Sci*, 1997, **110**, 861-870.
7. D. J. Geer and S. T. Andreadis, *J Invest Dermatol*, 2003, **121**, 1210-1216.
8. Y. Ikada, H. Iwata, T. Mita and S. Nagaoka, *J Biomed Mater Res*, 1979, **13**, 607-622.
9. H. R. Dickinson, A. Hiltner, D. F. Gibbons and J. M. Anderson, *J Biomed Mater Res*, 1981, **15**, 577-589.
10. A. J. Engler, S. Sen, H. L. Sweeney and D. E. Discher, *Cell*, 2006, **126**, 677-689.
11. B. Trappmann, J. E. Gautrot, J. T. Connelly, D. G. T. Strange, Y. Li, M. L. Oyen, M. A. C. Stuart, H. Boehm, B. J. Li, V. Vogel, J. P. Spatz, F. M. Watt and W. T. S. Huck, *Nat Mater*, 2012, **11**, 642-649.
12. J. H. Wen, L. G. Vincent, A. Fuhrmann, Y. S. Choi, K. C. Hribar, H. Taylor-Weiner, S. C. Chen and A. J. Engler, *Nat Mater*, 2014, **13**, 979-987.
13. D. Bryder, D. J. Rossi and I. L. Weissman, *Am J Pathol*, 2006, **169**, 338-346.
14. F. H. Gage, *Science*, 2000, **287**, 1433-1438.
15. N. L. Kennea and H. Mehmet, *J Pathol*, 2002, **197**, 536-550.
16. K. J. Lampe, R. G. Mooney, K. B. Bjugstad and M. J. Mahoney, *J Biomed Mater Res A*, 2010, **94a**, 1162-1171.
17. A. Banerjee, M. Arha, S. Choudhary, R. S. Ashton, S. R. Bhatia, D. V. Schaffer and R. S. Kane, *Biomaterials*, 2009, **30**, 4695-4699.
18. K. Saha, A. J. Keung, E. F. Irwin, Y. Li, L. Little, D. V. Schaffer and K. E. Healy, *Biophysical Journal*, 2008, **95**, 4426-4438.

19. A. Ribeiro, S. Vargo, E. M. Powell and J. B. Leach, *Tissue Engineering Part A*, 2012, **18**, 93-102.
20. Y. Mao and J. E. Schwarzbauer, *J Cell Sci*, 2005, **118**, 4427-4436.
21. J. L. Sechler, S. A. Corbett and J. E. Schwarzbauer, *Molecular Biology of the Cell*, 1997, **8**, 2563-2573.
22. K. J. Lampe, A. L. Antaris and S. C. Heilshorn, *Acta Biomater*, 2013, **9**, 5590-5599.
23. S.-H. Kim, J. Turnbull and S. Guimond, *Journal of Endocrinology*, 2011, **209**, 139-151.
24. W. P. Daley, S. B. Peters and M. Larsen, *J Cell Sci*, 2008, **121**, 255-264.
25. K. T. Tisay and B. Key, *Journal of Neuroscience*, 1999, **19**, 9890-9899.
26. R. J. McKeon, R. C. Schreiber, J. S. Rudge and J. Silver, *Journal of Neuroscience*, 1991, **11**, 3398-3411.
27. H. Lee, R. J. McKeon and R. V. Bellamkonda, *Proceedings of the National Academy of Sciences of the United States of America*, 2010, **107**, 3340-3345.
28. C. M. Williams, A. J. Engler, R. D. Slone, L. L. Galante and J. E. Schwarzbauer, *Cancer Res*, 2008, **68**, 3185-3192.
29. X. J. Tian, G. Rusanescu, W. M. Hou, B. Schaffhausen and L. A. Feig, *Embo J*, 2002, **21**, 1327-1338.
30. H. Xia, R. S. Nho, J. Kahm, J. Kleidon and C. A. Henke, *J Biol Chem*, 2004, **279**, 33024-33034.
31. R. McBeath, D. M. Pirone, C. M. Nelson, K. Bhadriraju and C. S. Chen, *Dev Cell*, 2004, **6**, 483-495.
32. P. J. Lein, D. Higgins, D. C. Turner, L. A. Flier and V. P. Terranova, *Journal of Cell Biology*, 1991, **113**, 417-428.
33. R. G. Jenkins, X. Su, G. Su, C. J. Scotton, E. Camerer, G. J. Laurent, G. E. Davis, R. C. Chambers, M. A. Matthay and D. Sheppard, *Journal of Clinical Investigation*, 2006, **116**, 1606-1614.
34. B. Heissig, K. Hattori, S. Dias, M. Friedrich, B. Ferris, N. R. Hackett, R. G. Crystal, P. Besmer, D. Lyden, M. A. S. Moore, Z. Werb and S. Rafii, *Cell*, 2002, **109**, 625-637.
35. M. Abercrombie and G. A. Dunn, *Experimental Cell Research*, 1975, **92**, 57-62.
36. A. D. Bershadsky, I. S. Tint, A. A. Neyfakh and J. M. Vasiliev, *Experimental Cell Research*, 1985, **158**, 433-444.
37. W. T. Chen and S. J. Singer, *Journal of Cell Biology*, 1982, **95**, 205-222.
38. B. Geiger, A. Bershadsky, R. Pankov and K. M. Yamada, *Nature Reviews Molecular Cell Biology*, 2001, **2**, 793-805.
39. O. P. Hamill and B. Martinac, *Physiological Reviews*, 2001, **81**, 685-740.
40. U. Muller and A. Littlewood-Evans, *Trends in Cell Biology*, 2001, **11**, 334-342.
41. T. Matsui, A. Raya, C. Callol-Massot, Y. Kawakami, I. Oishi, C. Rodriguez-Esteban and J. C. Izpisua Belmonte, *Nat Clin Pract Cardiovasc Med*, 2007, **4 Suppl 1**, S77-82.
42. W. F. Vogel, A. Aszodi, F. Alves and T. Pawson, *Mol Cell Biol*, 2001, **21**, 2906-2917.



43. A. Kanematsu, A. Marui, S. Yamamoto, M. Ozeki, Y. Hirano, M. Yamamoto, O. Ogawa, M. Komeda and Y. Tabata, *Journal of Controlled Release*, 2004, **99**, 281-292.
44. K. E. Kubow, E. Klotzsch, M. L. Smith, D. Gourdon, W. C. Little and V. Vogel, *Integrative Biology*, 2009, **1**, 635-648.
45. D. Perissinotto, P. Iacopetti, I. Bellina, R. Doliana, A. Colombatti, Z. Pettway, M. Bronner-Fraser, T. Shinomura, K. Kimata, M. Morgelin, J. Lofberg and R. Perris, *Development*, 2000, **127**, 2823-2842.
46. L. A. Davidson, B. D. Dzamba, R. Keller and D. W. Desimone, *Dev Dynam*, 2008, **237**, 2684-2692.
47. C. L. Zhong, M. Chrzanowska-Wodnicka, J. Brown, A. Shaub, A. M. Belkin and K. Burridge, *Journal of Cell Biology*, 1998, **141**, 539-551.
48. M. Yi and E. Ruoslahti, *Proceedings of the National Academy of Sciences of the United States of America*, 2001, **98**, 620-624.
49. E. P. S. Gee, D. Yueksel, C. M. Stultz and D. E. Ingber, *J Biol Chem*, 2013, **288**, 21329-21340.
50. F. S. Jones and P. L. Jones, *Dev Dynam*, 2000, **218**, 235-259.
51. M. Yamagata, K. M. Yamada, M. Yoneda, S. Suzuki and K. Kimata, *J Biol Chem*, 1986, **261**, 3526-3535.
52. K. M. Yamada, D. W. Kennedy, K. Kimata and R. M. Pratt, *J Biol Chem*, 1980, **255**, 6055-6063.
53. P. Pesheva, R. Probstmeier, A. P. N. Skubitz, J. B. McCarthy, L. T. Furcht and M. Schachner, *J Cell Sci*, 1994, **107**, 2323-2333.
54. L. Hakansson and P. Venge, *Journal of Immunology*, 1985, **135**, 2735-2739.
55. K. Wang, R. C. Andresen Equiluz, F. Wu, B. Ri Seo, C. Fischbach and D. Gourdon, *Biomaterials*, In Press.
56. M. Salmeron-Sanchez, P. Rico, D. Moratal, T. T. Lee, J. E. Schwarzbauer and A. J. Garcia, *Biomaterials*, 2011, **32**, 2099-2105.
57. W. R. Legant, C. S. Chen and V. Vogel, *Integrative Biology*, 2012, **4**, 1164-1174.
58. D. Seliktar, *Science*, 2012, **336**, 1124-1128.
59. K. J. Lampe, K. B. Bjugstad and M. J. Mahoney, *Tissue Engineering Part A*, 2010, **16**, 1857-1866.
60. J. M. Anderson and M. S. Shive, *Advanced Drug Delivery Reviews*, 1997, **28**, 5-24.
61. Y. W. Chun, D. A. Balikov, T. K. Feaster, C. H. Williams, C. C. Sheng, J. B. Lee, T. C. Boire, M. D. Neely, L. M. Bellan, K. C. Ess, A. B. Bowman, H. J. Sung and C. C. Hong, *Biomaterials*, 2015, **67**, 52-64.
62. K. B. Bjugstad, K. Lampe, D. S. Kern and M. Mahoney, *J Biomed Mater Res A*, 2010, **95A**, 79-91.
63. K. B. Bjugstad, D. E. Redmond, K. J. Lampe, D. S. Kern, J. R. Sladek and M. J. Mahoney, *Cell Transplantation*, 2008, **17**, 409-415.
64. J. J. Rice, M. M. Martino, L. De Laporte, F. Tortelli, P. S. Briquez and J. A. Hubbell, *Advanced Healthcare Materials*, 2013, **2**, 57-71.
65. T. S. Girton, T. R. Oegema, E. D. Grassl, B. C. Isenberg and R. T. Tranquillo, *Journal of Biomechanical Engineering-Transactions of the Asme*, 2000, **122**, 216-223.

66. C. Chung, K. J. Lampe and S. C. Heilshorn, *Biomacromolecules*, 2012, **13**, 3912-3916.
67. J. A. Andrades, B. Han, J. Becerra, N. Sorgente, F. L. Hall and M. E. Nimni, *Experimental Cell Research*, 1999, **250**, 485-498.
68. Y. H. Shen, M. S. Shoichet and M. Radisic, *Acta Biomater*, 2008, **4**, 477-489.
69. A. K. Lynn, I. V. Yannas and W. Bonfield, *Journal of Biomedical Materials Research Part B-Applied Biomaterials*, 2004, **71B**, 343-354.
70. F. Ruggiero and M. Koch, *Methods*, 2008, **45**, 75-85.
71. Y. S. Choi, S. R. Hong, Y. M. Lee, K. W. Song, M. H. Park and Y. S. Nam, *Biomaterials*, 1999, **20**, 409-417.
72. T. A. Holland, Y. Tabata and A. G. Mikos, *Journal of Controlled Release*, 2005, **101**, 111-125.
73. T. P. Ugarova and V. P. Yakubenko, *Fibrinogen*, 2001, **936**, 368-385.
74. M. W. Mosesson, *Journal of Thrombosis and Haemostasis*, 2005, **3**, 1894-1904.
75. J. Patterson, M. M. Martino and J. A. Hubbell, *Materials Today*, 2010, **13**, 14-22.
76. P. J. Johnson, S. R. Parker and S. E. Sakiyama-Elbert, *J Biomed Mater Res A*, 2010, **92A**, 152-163.
77. Y. C. Liu, S. Ahmad, X. Z. Shu, R. K. Sanders, S. A. Kopesec and G. D. Prestwich, *Journal of Orthopaedic Research*, 2006, **24**, 1454-1462.
78. S. Duflo, S. L. Thibeault, W. H. Li, X. Z. Shu and G. D. Prestwich, *Tissue Engineering*, 2006, **12**, 2171-2180.
79. C. M. Riley, P. W. Fuegy, M. A. Firpo, X. Z. Shu, G. D. Prestwich and R. A. Peattie, *Biomaterials*, 2006, **27**, 5935-5943.
80. P. Bulpitt and D. Aeschlimann, *J Biomed Mater Res*, 1999, **47**, 152-169.
81. G. D. Prestwich, *Journal of Controlled Release*, 2011, **155**, 193-199.
82. Y. D. Park, N. Tirelli and J. A. Hubbell, *Biomaterials*, 2003, **24**, 893-900.
83. J. Kim, Y. Park, G. Tae, K. B. Lee, S. J. Hwang, I. S. Kim, I. Noh and K. Sun, *Journal of Materials Science-Materials in Medicine*, 2008, **19**, 3311-3318.
84. B. G. Ballios, M. J. Cooke, D. van der Kooy and M. S. Shoichet, *Biomaterials*, 2010, **31**, 2555-2564.
85. T. Hashimoto, Y. Suzuki, M. Tanihara, Y. Kakimaru and K. Suzuki, *Biomaterials*, 2004, **25**, 1407-1414.
86. K. Lee, E. A. Silva and D. J. Mooney, *Journal of the Royal Society Interface*, 2011, **8**, 153-170.
87. R. T. Kershen, S. D. Fefer and A. Atala, *World Journal of Urology*, 2000, **18**, 51-55.
88. W. R. Gombotz and S. F. Wee, *Advanced Drug Delivery Reviews*, 1998, **31**, 267-285.
89. P. Eiselt, K. Y. Lee and D. J. Mooney, *Macromolecules*, 1999, **32**, 5561-5566.
90. J. A. Rowley, G. Madlambayan and D. J. Mooney, *Biomaterials*, 1999, **20**, 45-53.
91. N. H. Romano, K. J. Lampe, H. Xu, M. M. Ferreira and S. C. Heilshorn, *Small*, 2015, **11**, 722-730.
92. N. H. Romano, C. M. Madl and S. C. Heilshorn, *Acta Biomater*, 2015, **11**, 48-57.
93. K. M. Yamada, *J Biol Chem*, 1991, **266**, 12809-12812.

94. E. Ruoslahti, *Annual Review of Cell and Developmental Biology*, 1996, **12**, 697-715.
95. L. M. Weber, K. N. Hayda, K. Haskins and K. S. Anseth, *Biomaterials*, 2007, **28**, 3004-3011.
96. J. P. Jung, J. V. Moyano and J. H. Collier, *Integrative Biology*, 2011, **3**, 185-196.
97. J. W. Gunn, S. D. Turner and B. K. Mann, *J Biomed Mater Res A*, 2005, **72A**, 91-97.
98. L. Marquardt and R. K. Willits, *J Biomed Mater Res A*, 2011, **98A**, 1-6.
99. W. M. Tian, C. L. Zhang, S. P. Hou, X. Yu, F. Z. Cui, Q. Y. Xu, S. L. Sheng, H. Cui and H. D. Li, *Journal of Controlled Release*, 2005, **102**, 13-22.
100. J. Huynh, N. Nishimura, K. Rana, J. M. Peloquin, J. P. Califano, C. R. Montague, M. R. King, C. B. Schaffer and C. A. Reinhart-King, *Science Translational Medicine*, 2011, **3**.
101. R. G. Hibbs, *The American Journal of Anatomy*, 1956, **99**, 17-51.
102. F. Liu, J. D. Mih, B. S. Shea, A. T. Kho, A. S. Sharif, A. M. Tager and D. J. Tschumperlin, *Journal of Cell Biology*, 2010, **190**, 693-706.
103. J. L. Young and A. J. Engler, *Biomaterials*, 2011, **32**, 1002-1009.
104. J. L. Young, J. Tuler, R. Braden, P. Schup-Magoffin, J. Schaefer, K. Kretchmer, K. L. Christman and A. J. Engler, *Acta Biomater*, 2013, **9**, 7151-7157.
105. M. Guvendiren and J. A. Burdick, *Nature Communications*, 2012, **3**.
106. S. Khetan, M. Guvendiren, W. R. Legant, D. M. Cohen, C. S. Chen and J. A. Burdick, *Nat Mater*, 2013, **12**, 458-465.
107. C. N. Salinas and K. S. Anseth, *Biomaterials*, 2008, **29**, 2370-2377.
108. W. Li, R. Luo, X. Lin, A. D. Jadhav, Z. Zhang, L. Yan, C. Y. Chan, X. Chen, J. He, C. H. Chen and P. Shi, *Biomaterials*, 2015, **65**, 76-85.
109. A. M. Kloxin, A. M. Kasko, C. N. Salinas and K. S. Anseth, *Science*, 2009, **324**, 59-63.
110. A. M. Kloxin, M. W. Tibbitt, A. M. Kasko, J. A. Fairbairn and K. S. Anseth, *Advanced Materials*, 2010, **22**, 61-+.
111. D. R. Griffin, W. M. Weaver, P. O. Scumpia, D. Di Carlo and T. Segura, *Nat Mater*, 2015, **14**, 737-744.
112. L.-H. Han, J. H. Lai, S. Yu and F. Yang, *Biomaterials*, 2013, **34**, 4251-4258.
113. B. P. Purcell, D. Lobb, M. B. Charati, S. M. Dorsey, R. J. Wade, K. N. Zellars, H. Doviak, S. Pettaway, C. B. Logdon, J. A. Shuman, P. D. Freels, J. H. Gorman, III, R. C. Gorman, F. G. Spinale and J. A. Burdick, *Nat Mater*, 2014, **13**, 653-661.
114. M. Morpurgo, F. M. Veronese, D. Kachensky and J. M. Harris, *Bioconjugate Chemistry*, 1996, **7**, 363-368.
115. M. P. Lutolf, J. L. Lauer-Fields, H. G. Schmoekel, A. T. Metters, F. E. Weber, G. B. Fields and J. A. Hubbell, *Proceedings of the National Academy of Sciences of the United States of America*, 2003, **100**, 5413-5418.
116. D. Seliktar, A. H. Zisch, M. P. Lutolf, J. L. Wrana and J. A. Hubbell, *J Biomed Mater Res A*, 2004, **68A**, 704-716.
117. A. H. Zisch, M. P. Lutolf, M. Ehrbar, G. P. Raeber, S. C. Rizzi, N. Davies, H. Schmoekel, D. Bezuidenhout, V. Djonov, P. Zilla and J. A. Hubbell, *Faseb Journal*, 2003, **17**, 2260-+.

118. T. Tokatlian, C. T. Shrum, W. M. Kadoya and T. Segura, *Biomaterials*, 2010, **31**, 8072-8080.
119. S. E. Sakiyama-Elbert and J. A. Hubbell, *Journal of Controlled Release*, 2000, **65**, 389-402.
120. K. S. Straley and S. C. Heilshorn, *Soft Matter*, 2009, **5**, 114-124.
121. K. S. Straley and S. C. Heilshorn, *Frontiers in neuroengineering*, 2009, **2**, 9-9.
122. M. Ehrbar, S. C. Rizzi, R. G. Schoenmakers, B. San Miguel, J. A. Hubbell, F. E. Weber and M. P. Lutolf, *Biomacromolecules*, 2007, **8**, 3000-3007.
123. J. Patterson and J. A. Hubbell, *Biomaterials*, 2010, **31**, 7836-7845.
124. J. Patterson and J. A. Hubbell, *Biomaterials*, 2011, **32**, 1301-1310.
125. G. P. Raeber, M. P. Lutolf and J. A. Hubbell, *Biophysical Journal*, 2005, **89**, 1374-1388.
126. M. H. Zaman, L. M. Trapani, A. Siemeski, D. MacKellar, H. Y. Gong, R. D. Kamm, A. Wells, D. A. Lauffenburger and P. Matsudaira, *Proceedings of the National Academy of Sciences of the United States of America*, 2006, **103**, 10889-10894.
127. K. M. Galler, L. Aulisa, K. R. Regan, R. N. D'Souza and J. D. Hartgerink, *Journal of the American Chemical Society*, 2010, **132**, 3217-3223.
128. E. Nance, C. Zhang, T.-Y. Shih, Q. Xu, B. S. Schuster and J. Hanes, *Acs Nano*, 2014, **8**, 10655-+.
129. R. Tang, W. Ji, D. Panus, R. N. Palumbo and C. Wang, *Journal of Controlled Release*, 2011, **151**, 18-27.
130. Y. Bae, S. Fukushima, A. Harada and K. Kataoka, *Angewandte Chemie-International Edition*, 2003, **42**, 4640-4643.
131. H. S. Yoo, E. A. Lee and T. G. Park, *Journal of Controlled Release*, 2002, **82**, 17-27.
132. E. M. Bachelder, T. T. Beaudette, K. E. Broaders, J. Dashe and J. M. J. Frechet, *Journal of the American Chemical Society*, 2008, **130**, 10494-+.
133. Y. Bae, N. Nishiyama, S. Fukushima, H. Koyama, M. Yasuhiro and K. Kataoka, *Bioconjugate Chemistry*, 2005, **16**, 122-130.
134. W. Chen, P. Zhong, F. Meng, R. Cheng, C. Deng, J. Feijen and Z. Zhong, *Journal of Controlled Release*, 2013, **169**, 171-179.
135. H. Sun, B. Guo, R. Cheng, F. Meng, H. Liu and Z. Zhong, *Biomaterials*, 2009, **30**, 6358-6366.
136. R. M. Sawant, J. P. Hurley, S. Salmaso, A. Kale, E. Tolcheva, T. S. Levchenko and V. P. Torchilin, *Bioconjugate Chemistry*, 2006, **17**, 943-949.
137. E. R. Gillies and J. M. J. Frechet, *Bioconjugate Chemistry*, 2005, **16**, 361-368.
138. A. Napoli, M. Valentini, N. Tirelli, M. Muller and J. A. Hubbell, *Nat Mater*, 2004, **3**, 183-189.
139. M. K. Gupta, J. R. Martin, T. A. Werfel, T. Shen, J. M. Page and C. L. Duvall, *Journal of the American Chemical Society*, 2014, **136**, 14896-14902.
140. K. M. Poole, C. E. Nelson, R. V. Joshi, J. R. Martin, M. K. Gupta, S. L. C. Haws, T. E. Kavanaugh, M. C. Skala and C. L. Duvall, *Biomaterials*, 2015, **41**, 166-175.
141. K. Miyata, M. Oba, M. Nakanishi, S. Fukushima, Y. Yamasaki, H. Koyama, N. Nishiyama and K. Kataoka, *Journal of the American Chemical Society*, 2008, **130**, 16287-16294.

142. M. Sanjoh, K. Miyata, R. J. Christie, T. Ishii, Y. Maeda, F. Pittella, S. Hiki, N. Nishiyama and K. Kataoka, *Biomacromolecules*, 2012, **13**, 3641-3649.
143. T.-H. Ku, S. Sahu, N. M. Kosa, K. M. Pham, M. D. Burkart and N. C. Gianneschi, *Journal of the American Chemical Society*, 2014, **136**, 17378-17381.
144. S. L. Schor, I. Ellis, C. Dolman, J. Banyard, M. J. Humphries, D. F. Mosher, A. M. Grey, A. P. Mould and A. M. Schor, *J Cell Sci*, 1996, **109**, 2581-2590.
145. A. W. Feinberg and K. K. Parker, *Nano Letters*, 2010, **10**, 2184-2191.
146. K. J. Lampe and S. C. Heilshorn, *Neurosci Lett*, 2012, **519**, 138-146.

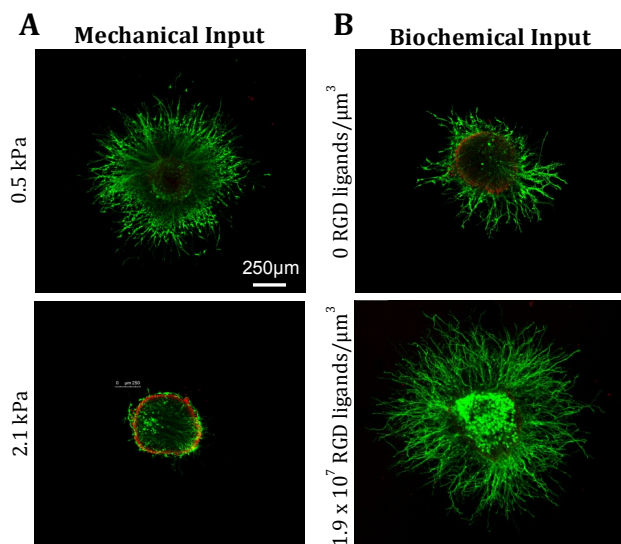
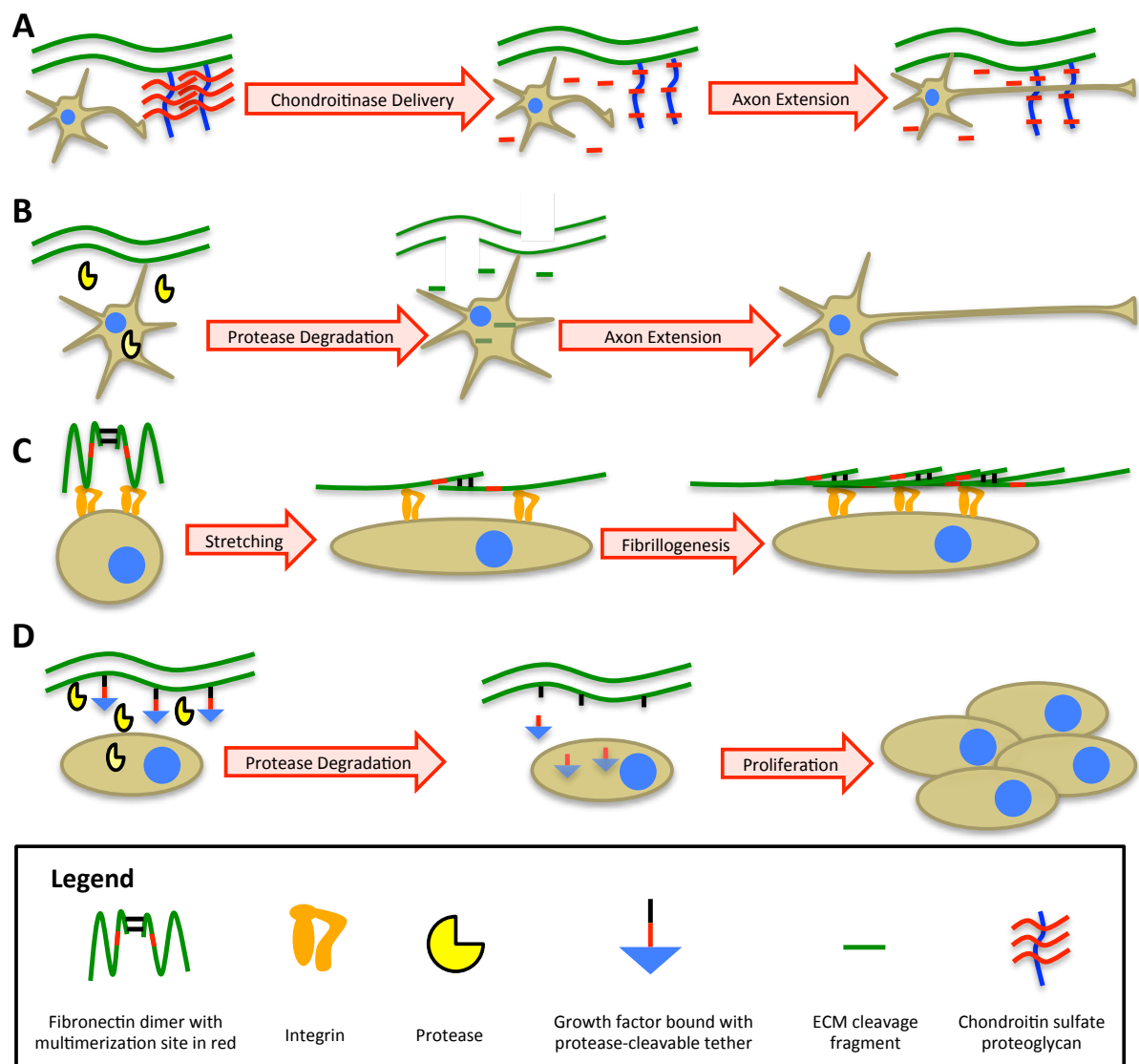
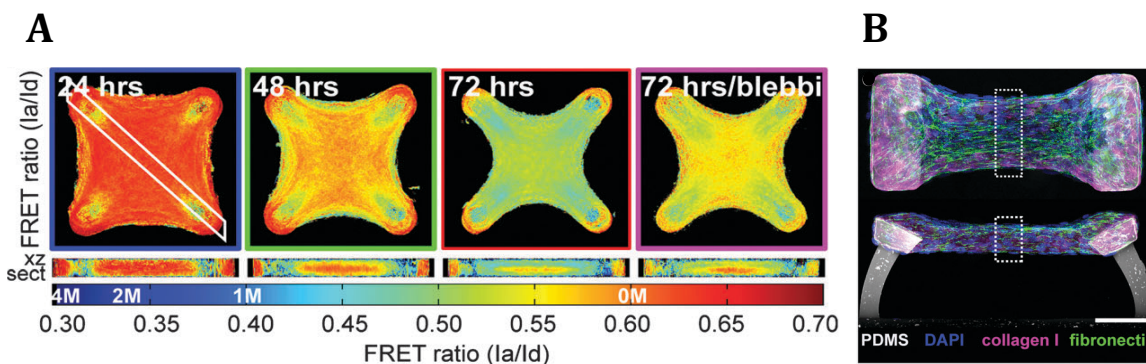


Figure 1. **Dorsal Root Ganglion (DRG) growth is dependent on mechanical and biochemical inputs.** (A) Maximized neurite outgrowth is seen in the ELP hydrogel (A) with stiffness mimicking the native neural environment ( $\sim 0.5$  kPa) and (B) incorporating the extended RGD adhesion sequence derived from fibronectin. Reproduced from Lampe *et al*<sup>22</sup>.





**Figure 2. Cell-ECM bidirectional communication inherent to tissue function can be engineered into tightly controlled designer biomaterials.** (A) CSPGs as part of the ECM are inhibitory to axon growth, a circumstance typically associated with the glial scar after CNS injury. Local chondroitinase delivery can be used to degrade the glycosaminoglycan thus allowing axon regrowth or new sprouting. (B) Cell-secreted proteases can degrade the ECM releasing fragments that act as signaling molecules. For example, the NC1 domain, a collagen degradation fragment, can enhance neurite outgrowth of DRGs. (C) Cells can stretch fibronectin upon binding via cell surface receptors. This stretching can reveal cryptic domains critical for fibronectin-fibronectin multimerization to result in fibril formation. (D) Cell-secreted proteases can release growth factors from the ECM leading to proliferation.



**Figure 3. Cells remodel and unfold fibronectin over space and time.** (A) Cells remodel an initial collagen scaffold by depositing and stretching fibronectin. FRET reveals increased fibronectin stretching over time and clear gradients in fibronectin stretching in the  $xy$  and  $xz$  planes of the microtissue.  $I_a$  refers to the acceptor fluorophore emission intensity, and  $I_d$  refers to the donor fluorophore emission intensity; higher FRET ratios correspond to less fibronectin stretching as indicated by warmer color. Blebbistatin treatment to eliminate cell-binding forces reveals that approximately 40% of fibronectin stretching is due to cellular contractility. (B) Fibronectin deposition onto an initial collagen scaffold corresponds to increasing matrix tension. Reproduced from Ref. 57 with permission from the Royal Society of Chemistry.

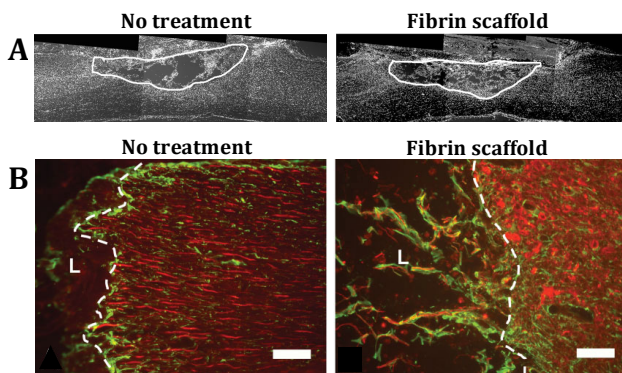


**Figure 4. Fibrin scaffold implantation promotes spinal cord regeneration after lesion.** (A) A nuclear stain shows that after spinal cord injury, implantation of a fibrin scaffold into the lesion site promotes cellular infiltration into the lesion. (B) In the fibrin-scaffold-treated group, neural fibers (Tuj1, red) penetrate through the glial border (GFAP, green) into the lesion site (marked L) and localize with GFAP-positive astrocytes. Reproduced from Johnson *et al*<sup>76</sup>.

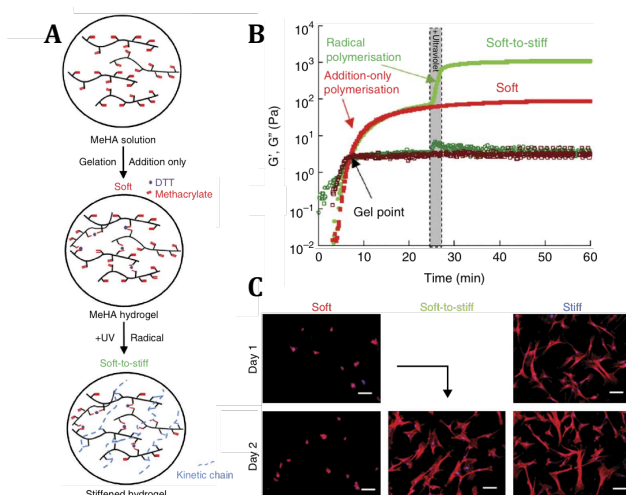


**Figure 5. Switch-like hydrogel stiffening induces phenotypic cellular changes.** (A) Methacrylated hyaluronic acid (MeHA) hydrogel is initially gelled by crosslinking with DTT. At a user-defined time point later, stiffening is induced by secondary crosslinking via UV light photoinitiation. (B) Rheological data show switch-like stiffening of Me-HA only with UV-initiated radical polymerization. (C) Morphology and cell area after the stiffness “switch” at one day of soft culture is similar to that of hMSCs cultured on the stiff material for the entire period. Reproduced from Guvendiren and Burdick<sup>105</sup>.

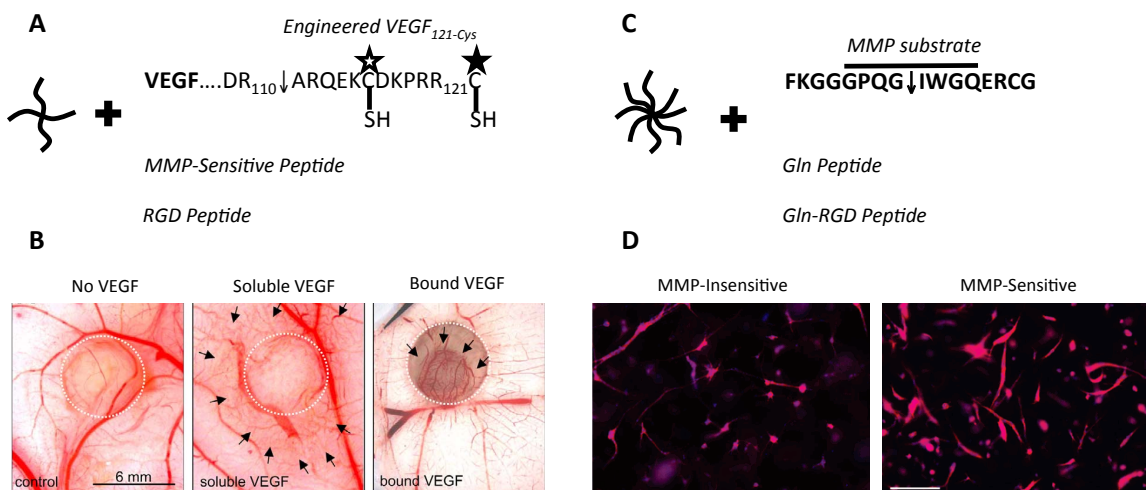


**Figure 6. Engineering matrix proteins with cell-induced degradability enhances implanted hydrogel regenerative potential.** (A) Exogenous cysteine residues were added to VEGF<sub>121</sub> such that the growth factor could be presented as a pendant molecule onto a PEG-VS scaffold crosslinked with free-thiol bearing, MMP-sensitive peptides also presenting RGD as a pendant molecule. The empty star indicates endogenous reactive cysteine. The filled star indicates exogenous reactive cysteine. (B) Neither the control hydrogel without VEGF nor the hydrogel with soluble VEGF elicited an angiogenic response after engraftment into a chicken chorioallantoic membrane (CAM) membrane. Conversely, the PEG hydrogel presenting VEGF bound to the scaffold via both MMP- and plasmin-sensitive tethers resulted in a highly localized angiogenetic response when grafted into a CAM membrane. Adapted from Zisch *et al*<sup>117</sup>. (C) Transglutaminase factor XIIIa was used to crosslink an engineered MMP-sensitive peptide with a glutamine donor (Gln) peptide and a fusion Gln-RGD peptide with PEG-CS. (D) Neonatal normal human dermal fibroblasts within MMP-sensitive gels show extensive spreading and form connections with other cells. Non-resorbable gels (MMP-insensitive) prevent cell spreading and organization. Adapted from Ehrbar *et al*<sup>122</sup>.

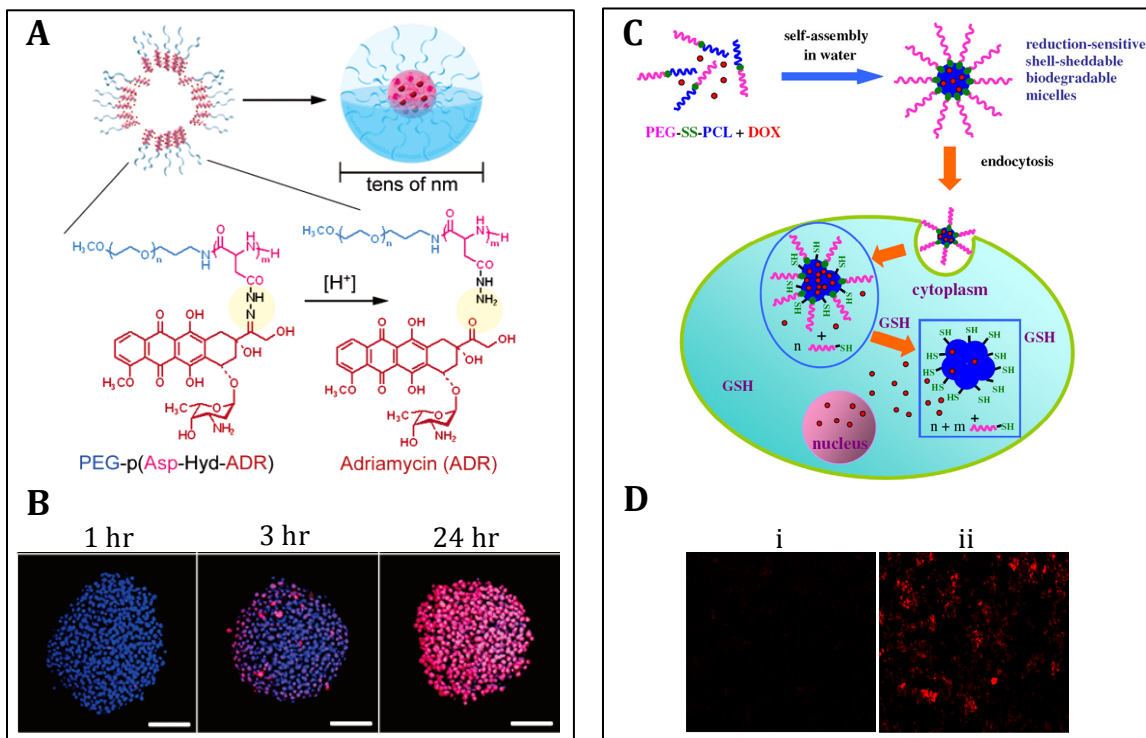
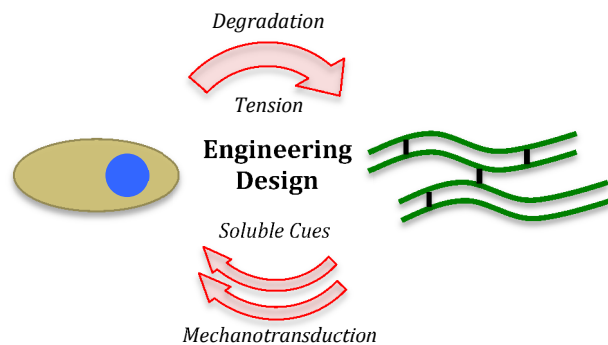


Figure 7. **Environment-responsive drug delivery vehicles support cell-mediated release.** (A) Micelles were formed from self-assembling polymers containing PEG, aspartate, and the anti-tumor drug adriamycin (ADR) where ADR was bound to aspartate by a pH-sensitive hydrazone bond, designed to release the payload upon the acidic tumor environment. (B) Micelles from (A) release their payload inside tumor cells (Nuclei-blue; ADR-pink). Reproduced from Bae *et al*<sup>133</sup>. (C) Reduction-sensitive micelles consisting of the diblock copolymer PEG-SS-PCL were designed to shed their PEG layer under reductive conditions such as high GSH concentrations indicative of the cytosol providing location-specific drug release. (D) Fluorescent microscopy of micelle uptake into mouse leukemic monocyte macrophage (RAW) cells after 2 hours shows that micelles rendered reduction-insensitive without the disulfide bond (i) released much less payload than reduction-sensitive micelles (ii). Reproduced from Sun *et al*<sup>135</sup>.





Statement of Novelty:

Novel methods to endow cell-responsiveness into hydrogels are explored and successful work is summarized.